



MAGIC: Motion-Aware Generative Inference via Confidence-Guided LLM

Siwei Meng

Department of Computer Science
University of Nevada Reno
Reno, NV 89512
siweim@unr.edu

Yawei Luo

School of Software Technology
Zhejiang University
Zhejiang, CN 310058
yaweiluo@zju.edu.cn

Ping Liu

Department of Computer Science
University of Nevada Reno
Reno, NV 89512
pino.pingliu@gmail.com

Abstract

Recent advances in static 3D generation have intensified the demand for physically consistent dynamic 3D content. However, existing video generation models, including diffusion-based methods, often prioritize visual realism while neglecting physical plausibility, resulting in implausible object dynamics. Prior approaches for physics-aware dynamic generation typically rely on large-scale annotated datasets or extensive model fine-tuning, which imposes significant computational and data collection burdens and limits scalability across scenarios. To address these challenges, we present MAGIC, a training-free framework for single-image physical property inference and dynamic generation, integrating pretrained image-to-video diffusion models with iterative LLM-based reasoning. Our framework generates motion-rich videos from a static image and closes the visual-to-physical gap through a confidence-driven LLM feedback loop that adaptively steers the diffusion model toward physics-relevant motion. To translate visual dynamics into controllable physical behavior, we further introduce a differentiable MPM simulator operating directly on 3D Gaussians reconstructed from the single image, enabling physically grounded, simulation-ready outputs without any supervision or model tuning. Experiments show that MAGIC outperforms existing physics-aware generative methods in inference accuracy and achieves greater temporal coherence than state-of-the-art video diffusion models.

1 Introduction

Realistic 3D content generation plays an essential role in immersive gaming environments and virtual simulations. Recent advancements in geometry and texture synthesis techniques [35, 34, 6, 32, 23] have significantly improved static 3D models. However, extending these successes to dynamic content generation remains challenging, particularly in ensuring rigorous physical consistency and semantic coherence in dynamic simulations. These dynamic generation challenges are also reflected in current diffusion-based video generation approaches [38, 25], which prioritize visual realism but often neglect the consistency of physical laws. As a result, generated dynamics often violate fundamental physical principles, such as conservation of mass and momentum, leading to artifacts like implausible component interactions, unstable linear motion trajectories, and inconsistent material

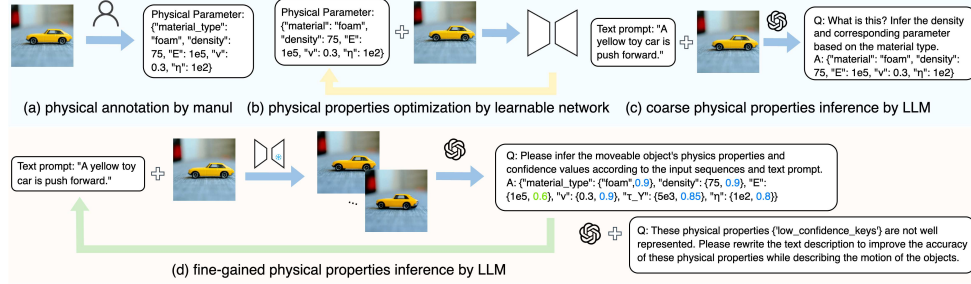


Figure 1: From Human Priors to Confidence-Guided LLM Feedback: A Comparison of Physical Property Inference Methods. (a) Human-annotated priors are inflexible and do not generalize to unseen objects. (b) Learning-based optimization require large annotated datasets and costly training. (c) LLM-based inference predicts approximate physical properties from language and visual input, but struggles with physical ambiguity and lacks fine-grained control. (d) Our iterative confidence-driven refinement enables precise estimation from minimal visual inputs. Blue arrow denotes forward reasoning; yellow arrow represents supervised optimization via labeled losses; green arrow indicates confidence-driven prompt refinement loop in MAGIC.

behaviors. These limitations degrade user immersion and hinder the application of generation models in physically sensitive simulation scenes.

The gap between visual realism and physical plausibility has motivated recent research into physically-aware generative methods [22, 16], which typically fall into two paradigms: (1) embedding physical priors directly into generative network architectures [37, 4] to ensure physical consistency at the expense of limited generalization, and (2) vision-based refinement approaches [19, 31, 20] that optimize outputs for physical realism from visual observations but heavily rely on extensive annotated data or suffer with perceptual ambiguities. Despite their progress, both paradigms share a critical bottleneck in precisely inferring physically consistent properties due to the inherent insufficiency of information from minimal visual inputs, such as a single static image. While manual priors such as PhysGaussian [36] have limitations in adaptability (Fig. 1a), learning-based estimators [3, 40, 17] typically require substantial datasets and computational resources (Fig. 1b). Recent LLM-based methods [19, 20] (Fig. 1c), although promising for high-level reasoning, often face challenges related to precision and ambiguity when relying on sparse visual cues.

In this paper, for the first time, we propose a novel, fully training-free vision-based framework that uniquely integrates pretrained diffusion-based video generation with confidence-driven, iterative LLM-guided feedback to achieve precise and reliable physical property inference from single static image. Our key insight is that combining the reasoning ability of LLM with and visual generation diversity of pre-trained video generation model can overcome the ambiguity of single image inputs. As illustrated in Fig. 2, “squeeze” motion of a toy car yield more accurate mass inference than “bomb” motion-revealing that motion diversity is crucial for acquiring optimized physical properties.

Motivated by this observation that different motion types provide varying level of physical evidence for property reasoning, our approach first leverages a pretrained image-to-video diffusion model [38] to synthesize informative motion-rich videos from single static images, significantly enriching visual cues necessary for robust inference. Recognizing that distinct physical properties (e.g., density, elasticity, mass) require specific motion contexts for optimal inference, we innovatively introduce an iterative visual-physical feedback mechanism powered by a large language model [2]. This mechanism evaluates initial property inference results with computed confidence scores, dynamically and adaptively refining textual prompts to regenerate videos explicitly tailored for accurate estimation of previously uncertain properties. Our work further integrates an MPM-based simulation engine [8], where we initialize the material points directly from 3D Gaussians reconstructed by a pretrained 3D Gaussian Splatting network [35] to achieve real-time simulation with near-interactive latency. Crucially, our uniquely designed training-free iterative mechanism substantially advances physics-aware generative modeling by dramatically improving inference accuracy and generalization without relying on any annotated datasets or computationally demanding fine-tuning processes.

Our main contributions are summarized as follows:

- We propose the first fully training-free visual-physical inference framework that integrates pretrained diffusion-based video generation and confidence-driven iterative LLM-guided

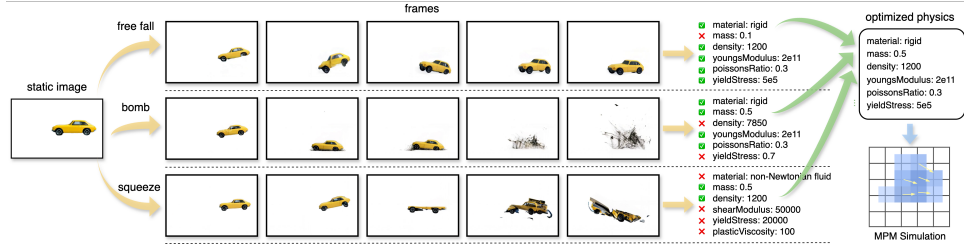


Figure 2: Static input image and generated motion sequences with the guidance of different motion types can yield distinct physical properties. For a static car input, with three motion (“free fall”, “bomb”, and “squeeze”) guidance, the output videos are suitable for distinct physics reasoning. Video generation and physical reasoning models in this setting are CogVideoX [38] and GPT-4o [2].

feedback, enabling precise and robust inference of intrinsic physical properties (e.g., density, elasticity, mass) from a single static image, without annotated data or supervised fine-tuning.

- We introduce a novel iterative LLM feedback mechanism that, for the first time, adaptively leverages computed confidence scores from initial inference to dynamically refine textual prompts, synthesizing targeted, informative videos specifically optimized to significantly enhance the precision and reliability of inferring uncertain physical properties.
- We demonstrate through extensive quantitative and qualitative experiments that our approach achieves superior accuracy, robustness, and generalization performance compared to existing state-of-the-art methods, particularly excelling in challenging scenarios involving physical inference from sparse visual inputs, thereby significantly reducing computational barriers and enhancing practical applicability.

2 Related Works

3D Dynamic Generation. Benefiting from advances in static 3D representation methods, recent dynamic 3D generation approaches [15, 29] extend static representations into temporal sequences by explicitly modeling object trajectories or applying deformation fields. Neural implicit-based methods [7, 26] integrate spatial coordinates, timestamps, and viewing directions through learned networks to achieve photorealistic novel-view synthesis in dynamic scenarios. However, these methods generally require high computational resources due to their reliance on voxel-based rendering. Recent developments in 3D Gaussian Splatting (3DGS) [10] enable real-time rendering, with extensions [9] capable of limited geometric deformations. Nevertheless, these approaches often overlook explicit physical modeling, potentially resulting in dynamics that lack physical realism.

Physics-Grounded Generative Models. Ensuring physically consistent dynamic generation has prompted explorations into physics-grounded generative models. Physically embedded generative networks [37, 4] explicitly integrate physical constraints, such as elasticity, density, and collision responses, into network architectures to produce physically plausible outputs. However, these approaches typically involve task-specific or material-dependent designs, potentially restricting their generalization capabilities. Alternatively, vision-based refinement frameworks [19, 20, 31] decouple visual generation from physical reasoning by first synthesizing dynamics using standard generative models and subsequently refining them via physics-based objectives. While offering flexibility across various scenarios, these methods may encounter optimization challenges, limited physical supervision during the initial generation phase, and difficulties in precisely controlling detailed physical attributes.

Large Language Model Reasoning. Inferring physical attributes from sparse visual inputs remains challenging for physics-aware modeling. Traditional approaches [36, 31, 40] often rely on supervised regression using extensively annotated video datasets, which require considerable annotation effort. Recently, large language models [2] have demonstrated promise for physical reasoning tasks by leveraging implicit knowledge of materials and motion behaviors. Methods like PhysGen [19] and PhysFlow [20] infer properties such as mass, elasticity, and force directions from static images; however, these approaches may experience reduced accuracy due to insufficient temporal context. Auxiliary synthetic video generation [38] enriches motion contexts but may not always ensure physically coherent dynamics, potentially affecting inference quality. To overcome these fundamental limitations, we propose, for the first time, an iterative prompting framework that leverages confidence-

driven LLM feedback to adaptively and dynamically optimize video generation in a fully training-free manner, significantly enhancing motion coherence and precision in physical property inference from minimal visual cues without updating any model parameters.

3 Preliminary

In this section, we briefly introduce essential background knowledge and notation that will be used throughout this paper. Specifically, we review 3D Gaussian Splatting, Continuum Mechanics, and the Material Point Method.

3D Gaussian Splatting (3DGS). 3D Gaussian Splatting [11] is a novel explicit 3D scene representation method that models scenes as a collection of anisotropic Gaussian kernels $\{x_k, \Sigma_k, \alpha_k, c_k\}, k \in \mathcal{K}$, encoding position, covariance matrix, opacity, and view-dependent color. Unlike implicit neural representations [24, 39], 3DGS features fully differentiable rasterization rendering process, and the pixel color $C(u)$ is computed via alpha blending of depth-sorted Gaussians:

$$C(u) = \sum_{k \in \mathcal{P}(u)} \alpha_k \mathcal{G}_k(u) \text{SH}(d_k; c_k) \prod_{j < k} (1 - \alpha_j \mathcal{G}_j(u)), \quad (1)$$

where $\mathcal{G}_k(u)$ is the current gaussian projection at pixel u , and SH denotes spherical harmonics for view-dependent colors c_k of viewing direction d_k . 3DGS provides directly optimizable properties where every Gaussian kernel can be individually modified to achieve efficient deformations.

Continuum Mechanics and Material Point Method. We model material behaviors using continuum mechanics [8, 28] that describes local deformation by a deformation map $\phi(\mathbf{X}, t)$, relating initial coordinates \mathbf{X} to current positions $\mathbf{x} = \phi(\mathbf{X}, t)$. For numerical simulation, we employ the Material Point Method (MPM) [8, 42], is a hybrid Lagrangian-Eulerian approach for solving continuum mechanics problems. MPM combines the accuracy of particle-based methods with the computational stability of Eulerian grids. The material is discretized into a set of Lagrangian particles $\{\mathbf{x}_p, m_p, \mathbf{v}_p, \mathbf{F}_p\}_{p=1}^N$, where m_p is mass, \mathbf{v}_p is velocity, and \mathbf{F}_p is the deformation gradient. Eulerian grids are used as intermediate structures to efficiently compute forces and spatial derivatives.

In MPM, each simulation step consists of three phases: (1) particle-to-grid (P2G) transfer, where mass and momentum are interpolated from particles to grid nodes; (2) grid update, where nodal velocities are computed by solving the discretized momentum equations under internal and external forces; and (3) grid-to-particle (G2P) transfer, where updated grid quantities are mapped back to particles to update their velocities, positions, and deformation gradients. This hybrid formulation enables MPM to handle large deformations, collisions, and multi-material interactions while maintaining numerical stability and physical accuracy.

4 Methodology

We propose **MAGIC**, a training-free framework for inferring physical properties and simulating physically plausible 3D dynamics from a single image. As illustrated in Fig. 3, MAGIC consists of two key stages: (1) a *physics perception stage*, which infers object-level physical parameters within an LLM-guided iterative video reasoning loop, and (2) a *physics-grounded dynamic stage*, which simulates time-varying 3D motion using a differentiable MPM solver operating on Gaussians. By integrating diffusion-based video generation, confidence-driven prompt refinement, LLM-based reasoning, and volumetric particle simulation into a unified pipeline, MAGIC closes the gap between visual motion and physical fidelity using only a few descriptive prompts for guidance.

4.1 Physics Perception Stage

The physics perception stage learns visual observation with physical understanding by extracting object-level physical properties from a single static image. Specifically, this stage consists of three component: (1) Image-to-Video Generation that enriches visual cues for subsequent reasoning, (2) LLM-Based Physics Reasoning that combines the reasoning ability to obtain physical parameters without training or manually setting, and (3) Confidence-Driven Prompt Reasoning that refines the physical understanding through the confidence feedback iterations.

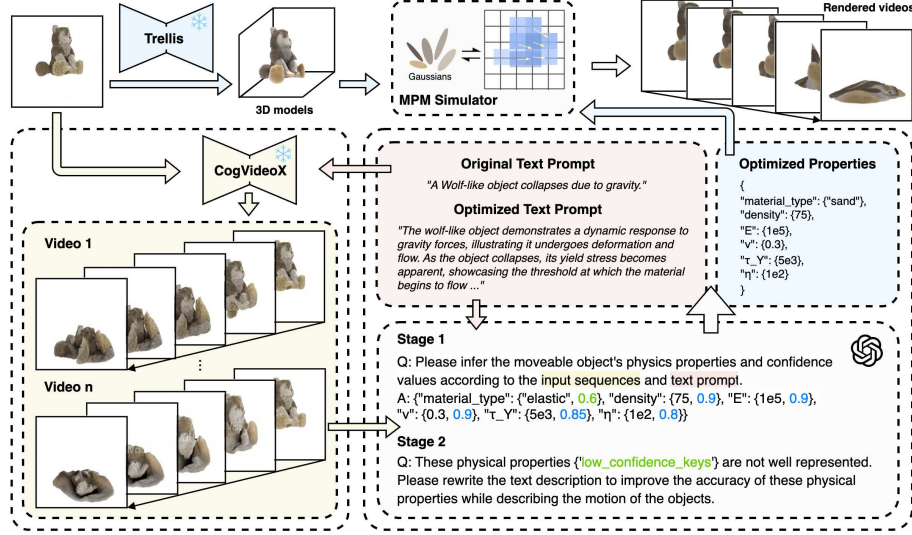


Figure 3: Overview framework of our method. MAGIC consists of two stages, Physics Perception and Physics-Grounded Dynamic. Physics Perception Stage utilizes pre-trained video generation models and LLM to obtain optimized physical properties. Physics-Grounded Dynamic Stage combines optimized physical properties into 3D models with MPM simulator to generate rendered videos.

Image-to-Video Generation. Given a single input image I_0 and an initial descriptive prompt, we generate a video sequence $V_0 = \{I_0, I_1, \dots, I_T\}$ using CogVideoX1.5-5B [38], a pretrained transformer-based diffusion model. We optionally subsample the video using a motion-aware sampling ratio α to remove redundant frames and retain informative motion cues. Compared to static images, temporal dynamics in video provide richer information for physical reasoning. For example, object mass, material, or external forces are often difficult to infer from a single frame, particularly when dealing with synthetic scenes such as PAC-NeRF [14], but become more observable through motion patterns. These synthesized video sequences thus serve as input for the subsequent LLM-based inference stage, where physical properties are estimated by reasoning over visual dynamics.

LLM-Based Physics Reasoning. While synthesized videos provide richer temporal dynamics than static images, accurately inferring physical properties directly from visual data remains challenging due to limited available annotations and the complexity of physics-aware reasoning. Existing pretrained LLMs, though capable of leveraging implicit knowledge, are not explicitly trained for physics tasks, often resulting in unreliable or ambiguous predictions. To address these challenges, we propose a structured coarse-to-fine inference framework using GPT-4o [2], which integrates pseudo-video generation with targeted descriptive prompts for robust physics inference.

As illustrated in Stage 1 of Fig. 3, our LLM-based reasoning process follows a structured three-stage pipeline: first, the LLM identifies the primary movable object within the generated video. Next, it classifies this object into a specific material category (e.g., sand, metal, or elastic) based on combined visual and textual cues. Finally, based on the identified material type, the LLM estimates fine-grained physical attributes, including static parameters P_s (e.g., mass, density, and elasticity) and dynamic parameters P_d (e.g., external forces and initial velocity). Each inferred attribute is also associated with a confidence score $c_i \in [0, 1]$, facilitating subsequent prompt refinement for uncertain predictions. Low-confidence predictions indicate uncertainty or video-text mismatch, which we explicitly handle via subsequent prompt refinement. The detailed query prompt can be found in the supplementary.

Confidence-Driven Prompt Refinement. Since direct LLM predictions may contain uncertainties due to misalignment between prompts and generated motion, relying solely on initial inferences can lead to physically inaccurate or ambiguous attribute estimations, as illustrated in Fig. 4, the carnation is incorrectly classified into non-newtonian fluid material due to the To robustly mitigate this limitation, we introduce an adaptive, confidence-guided refinement loop that strategically adjusts generation prompts to enhance motion relevance for uncertain physical attributes. Specifically, we define a confidence threshold γ and identify attributes P_i whose inferred confidence scores fall below this threshold. We first mark low-confidence attributes with:

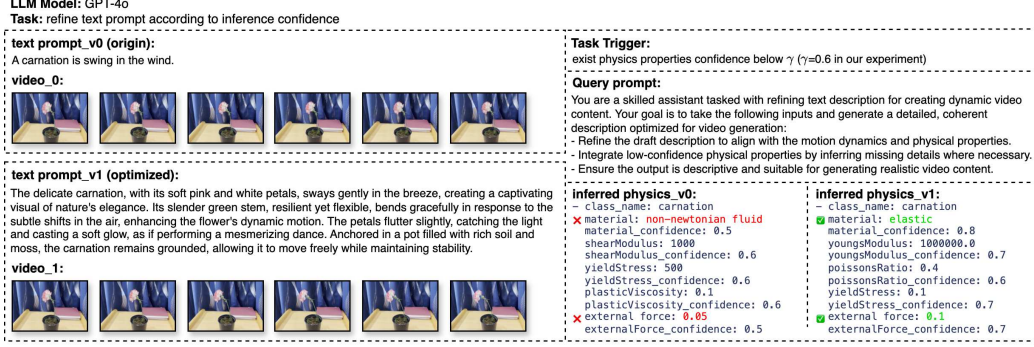


Figure 4: Confidence-driven text prompt refinement process. The presented *swing carnation* scene shows the comparison of an initial and optimized text prompt for optimized physics properties reasoning.

$$m_i = \begin{cases} 1, & c_i < \gamma, \\ 0, & c_i \geq \gamma, \end{cases} \quad (2)$$

where all indices i with $m_i = 1$ form the set of attributes needing refinement. Starting from the initial prompt $p^{(0)}$, we apply an update $p^{(t)}$ at iteration t as follows:

$$p^{(t+1)} = \text{LLM}(p^{(t)}, \{P_i | m_i = 1\}). \quad (3)$$

The LLM receives current text prompt $p^{(t)}$ and the corresponding low-confidence sets, inferring weak details for these attributes and outputs an updated prompt $p^{(t+1)}$. Whenever the low-confidence set is not empty, we iteratively optimize the text prompts to regenerate videos featuring more informative motion patterns, for instance, generating “free-fall” motion to accurately infer mass or gravity, or “burning” scenarios to better determine material types and melting points. As shown in Fig. 4, this iterative prompt-motion refinement continues until all physical attributes surpass the defined confidence threshold, significantly improving inference robustness. More detailed prompt templates and refinement strategies are provided in supplementary.

4.2 Physics-Grounded Dynamic Stage

The inferred physical properties from our LLM-guided iterative prompting provide essential priors for realistic dynamic simulation, yet transforming these abstract attributes into actionable 3D dynamics remains challenging. Existing single-image methods are inherently limited by the lack of accurate volumetric modeling, compromising their capability to simulate complex non-planar motions and intricate object-material interactions. To address these challenges, we propose the physics-grounded dynamic stage, which explicitly bridges the gap between inferred physics and volumetric simulation. Specifically, we reconstruct a precise 3D representation directly from the single input image and integrate the inferred physical attributes into a differentiable MPM solver, achieving physically coherent and controllable 3D dynamics.

Single Image to 3D Generation. Generating dynamics from a single image [19] remains challenging, especially for non-planar motion and scenarios involving complex object-material interactions. Conventional image-level simulation methods [30, 5] often neglect intrinsic material properties, resulting in unrealistic behaviors. Additionally, the lack of explicit volumetric modeling in single-image methods typically leads to inaccurate 3D geometry, particularly when simulating object deformation. To address these limitations and effectively bridge inferred physics with accurate dynamic simulation, we reconstruct a volumetric 3D representation from the single input image using a pretrained 3DGS model [35]. This model generates structured Gaussian kernels by combining sparse voxel features with multi-view visual encoding, providing high-fidelity reconstruction results. Each Gaussian kernel $G_k = (x_k, \Sigma_k, \alpha_k, c_k)$ serves as a material-carrying particle, directly facilitating the integration of inferred physical properties into subsequent simulation processes.

MPM-based 3D Dynamic Simulation. While existing differentiable simulators [1, 13, 41] typically target specific material types and lack mechanisms to integrate externally inferred physical attributes, our key insight is that explicitly coupling inferred physical properties with differentiable volumetric

simulation significantly improves both realism and controllability. Motivated by recent advances in differentiable physics modeling [36], we adopt a differentiable Material Point Method (MPM) framework capable of robustly modeling diverse material behaviors, including sand, elastic solids, jelly-like materials, metals, and plasticine. Crucially, instead of manually specifying physical parameters, we directly initialize particle states from our inferred Gaussian-based representations, effectively bridging physics inference and simulation within a unified differentiable framework. Specifically, each particle state at time step t is represented as:

$$\mathcal{G}_p^t = (x_p^t, \Sigma_p^t, \alpha_p, c_p, \theta_p^t), \quad (4)$$

where θ_p^t contains inferred properties such as mass, density, and material-specific parameters. During simulation, particle states, including positions x_p^t , velocities v_p^t , and deformation gradients \mathbf{F}_p^t , are updated via MPM dynamics:

$$v_p^{t+1} = v_i^{t+1}, \quad x_p^{t+1} = x_p^t + \Delta t v_p^{t+1}, \quad \mathbf{F}_p^{t+1} = (\mathbf{I} + \Delta t \nabla v_p) \mathbf{F}_p^t, \quad (5)$$

where i and p represent Eulerian grid and Lagrangian field respectively; Δt is the time step size; x_p^{t+1} denotes position of particle at time step $t + 1$, and v_p^{t+1} means particle velocity transferred from grid velocity field v_i^{t+1} ; $\mathbf{I} = \mathbf{F}_p^0$ represents the initial undeformed state; The velocity gradient ∇v_p ensures local deformation consistency. This process generates physically consistent dynamics directly from a single image, with explicit control of material-specific behaviors. By directly integrating LLM-inferred attributes into the differentiable MPM solver, our approach not only maintains simulation realism but also enables explicit control of complex dynamic behaviors from minimal visual input. This tight integration between physics inference and differentiable simulation represents a significant departure from prior methods, facilitating more versatile and physically coherent dynamic generation.

In summary, MAGIC uniquely unifies training-free, LLM-driven physics reasoning with differentiable volumetric simulation, enabling precise and controllable 3D dynamics directly from a single image. By iteratively refining physical priors through confidence-guided LLM feedback, and explicitly coupling these inferred attributes with a differentiable MPM solver initialized from high-fidelity Gaussian representations, MAGIC surpasses prior approaches in accuracy, flexibility, and physical realism—all without relying on annotated datasets or task-specific fine-tuning.

5 Experiments

5.1 Experimental Setup

Implementation Details. Our implementation is fully training-free, integrating several pretrained models to enable efficient and robust dynamic generation without requiring additional fine-tuning or task-specific supervision. For the initial 3D reconstruction, we employ Trellis [35] to obtain high-fidelity 3D Gaussian representations. For video generation to support effective physics inference, we use CogVideoX-5b model [38], and the generated videos are 720×480 with 50 frames. To reduce visual redundancy in subsequent LLM [2] reasoning, we subsample 6-8 representative frames per sequence. The number of iterations for confidence-driven prompt refinement is fixed to 3, ensuring a balance between inference robustness and computational efficiency. The physics-based dynamic simulation is implemented using a differentiable MPM solver [36] integrated within the Warp simulation framework [21], configured with 128-200 simulation steps per dynamic sequence. All experiments are conducted on a single NVIDIA RTX 4090 GPU with 24GB memory.

Benchmark. We conduct extensive experiments to evaluate our method, primarily on the real-world datasets introduced by PhysGaussian [36] and PhysGen [19]. To further demonstrate the generality of our approach, we also utilize several static images (e.g., rolling basketball and sway tree) collected from the Internet for qualitative evaluation. Our evaluation adopts three different metrics: (1) CLIP Similarity (\mathbf{C}_{sim}) [27] measuring video-text prompt alignment; (2) Aesthetic quality score (\mathbf{A}_{score}) [12] assessing per-frame visual quality; (3) Physical plausibility and text consistency of dynamic 3D assets through a user study. For the user study, we collect ratings from 61 participants on 32 videos generated by four methods. The videos were presented in random order, and participants evaluated them on a 4-point Likert scale (1 = least consistent, 4 = most consistent) based on physical plausibility and text consistency, providing a comprehensive measure of human preference.

Table 1: Quantitative evaluation across eight scenarios on C_{sim} (semantic alignment, higher better) and A_{score} (physical accuracy, higher better) metrics. Best results in each scenario are highlighted in **bold**.

Method	Swing ficus		Sand wolf		Driving car		Rolling basketball		Tear toast		Sway tree		Lifting hat		Swing carnation		Avg.	
	C_{sim}	A_{score}	C_{sim}	A_{score}	C_{sim}	A_{score}	C_{sim}	A_{score}	C_{sim}	A_{score}	C_{sim}	A_{score}	C_{sim}	A_{score}	C_{sim}	A_{score}	C_{sim}	A_{score}
OpenSora2.0	0.270	27.26	0.264	14.58	0.195	5.51	0.230	17.74	0.274	23.85	0.174	17.44	0.239	2.53	0.217	26.97	0.233	16.98
CogVideoX	0.279	33.19	0.225	22.55	0.241	38.55	0.226	11.91	0.250	47.18	0.186	21.51	0.252	16.37	0.254	54.02	0.239	30.66
CogVideoX*	0.257	34.89	0.263	23.94	0.234	41.20	0.233	17.95	0.279	46.49	0.195	22.53	0.241	16.41	0.254	51.47	0.240	31.86
Ours	0.294	31.00	0.200	18.38	0.252	29.40	0.266	26.82	0.231	49.85	0.243	39.67	0.270	26.74	0.256	23.70	0.251	30.69

Table 2: Quantitative results on CLIP similarity with physics-aware generation methods across two challenging scenes.

Scene	PhysDreamer	Physics3D	OMNIPHYSGS	Ours
Swing ficus	0.223	0.225	0.227	0.294
Sand wolf	0.145	0.147	0.167	0.200

Table 3: Quantitative results of human evaluation on physical plausibility and text consistency across eight real-world scenes.

Metric	OpenSora2.0	CogVideoX	CogVideoX*	Ours
Physical Plausibility	2.02	2.58	2.97	3.00
Text Consistency	2.18	2.49	3.00	3.07

Baseline Models. We compare our approach extensively with representative state-of-the-art methods, covering both video generation models [38, 25] and physics-aware 3D dynamic generation approaches. CogVideoX [38] represents a diffusion-based image-to-video generation framework that achieves stable and visually coherent motion through multi-scale temporal attention. OpenSora 2.0 [25] is an open-source video generation model that leverages hierarchical diffusion with spatiotemporal conditioning to synthesize high-quality sequences. As an ablation study, we also evaluate CogVideoX* with enhancement by our confidence-driven prompt refinement module. For physics-aware generation baselines, we compare with PhysDreamer [40], Physics3D [18], and OMNIPHYSGS [17]. PhysDreamer learns physical properties from current video diffusion models, and Physics3D [18] integrates viscoelastic MPM with Score Distillation Sampling to simulate multi material behaviors. OMNIPHYSGS [17] provides a physics-based 3D dynamic synthesis framework capable of modeling diverse material behaviors.

5.2 Quantitative Results

Table 1 quantitatively compares our MAGIC against state-of-the-art baselines, including OpenSora2.0, CogVideoX, and CogVideoX* across eight diverse scenarios. Our method consistently achieves superior C_{sim} scores in most scenarios, demonstrating stronger semantic alignment between generated motions and textual prompts. Specifically, MAGIC attains the highest average C_{sim} of 0.251, notably outperforming OpenSora2.0 (0.233), CogVideoX (0.239), and CogVideoX* (0.240). While CogVideoX* obtains a slightly higher average A_{score} (31.860 vs. our 30.694), MAGIC achieves significantly better A_{score} and C_{sim} performance in key challenging scenarios such as *rolling basketball*, *lifting hat*, and *sway tree*. Additionally, Table 2 compares MAGIC with state-of-the-art physics-aware baselines on two representative challenging scenarios. MAGIC establishes statistically improvement than baseline models, with 0.294 and 0.200 on both elastic (*swing ficus*) and sand (*sand wolf*) scenarios. This reflects MAGIC’s unique capability to simultaneously maintain high visual quality and accurate text-motion coherence, highlighting the effectiveness of our iterative LLM-guided refinement in synthesizing physically plausible and semantically consistent dynamics.

We further validate the effectiveness of MAGIC through a human-centered user study evaluating physical plausibility and text consistency. As reported in Table 3, MAGIC achieves the highest ratings in both metrics, scoring 3.00 for physical plausibility and 3.07 for text consistency. CogVideoX* closely follows with scores of 2.97 and 3.01, significantly outperforming both CogVideoX and OpenSora2.0. The noticeable improvement from CogVideoX to CogVideoX* highlights the effectiveness of our confidence-driven prompt refinement strategy, clearly enhancing both dynamic realism and semantic alignment. Overall, these user study results strongly indicate MAGIC’s superior capability in producing physically plausible and semantically consistent dynamic content.

5.3 Qualitative Results

In our comparative evaluation with state-of-the-art video generation models, as illustrated in Fig. 5, our method exhibits distinct advantages in modeling physically realistic dynamics given only a static image, while both OpenSora 2.0 [25] and CogVideoX [38] generate videos with visual distortion

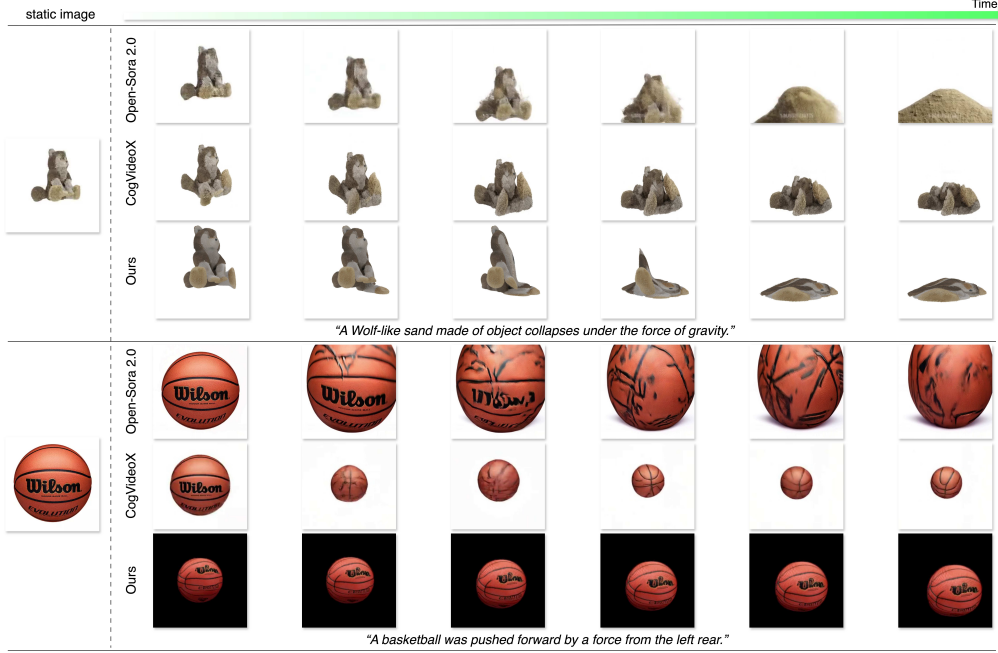


Figure 5: Qualitative comparisons of dynamic scene generation between our method and state-of-the-art video generation models [25, 38]. Given only a single static image (leftmost), our approach effectively infers intrinsic physical properties and generates highly realistic dynamics over time (left to right), demonstrating superior physical realism and temporal consistency.

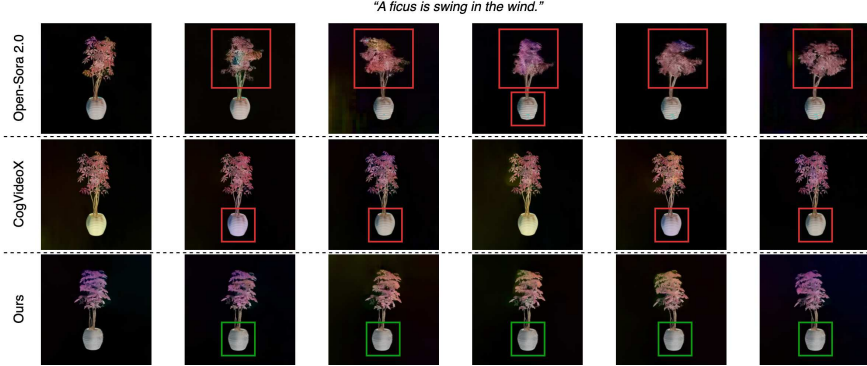


Figure 6: Qualitative comparison of optical flow visualization between our method and state-of-the-art video generation models [25, 38]. We evaluate the optical flows between generated motions of *swing ficus*. Our method exhibits superior physical controllability and structural stability over time, effectively maintaining coherent motion without significant distortion (highlighted in green boxes). In contrast, competing methods suffer from visible structural inconsistencies and unnatural shape distortions (highlighted in red boxes).

and physical anomalies. For the wolf-like sand collapse, Open-Sora 2.0 and CogVideoX exhibit unnatural particle scattering behaviors, while our results correctly simulate sand material behavior under gravity. In the *rolling basketball* scene, baseline models produce implausible deformations under external forces or distorted appearance with origin input image, whereas our method maintains consistent appearance and motion.

Fig. 6 visualizes estimated optical flow [33] on a sample *swing ficus* scene. OpenSora2.0 exhibits spurious edges and temporal jitter around movable regions, indicating weak motion coherence, and the bottom vase also shows slight deformation. Both MAGIC and CogVideoX illustrate stable optical flow, however, CogVideoX lacks precise spatial control over motion regions. Specifically, CogVideoX generates unintended motion flow in the static vase region due to its global motion modeling strategy. Our method achieves accurate motion localization through physics-aware constraints, ensuring only the target regions exhibit dynamic deformation while maintaining stability in static objects.

Furthermore, our framework explicitly models motion trends by integrating physical priors, resulting in obvious dynamics compared to the data-driven baselines.

6 Conclusions

We present MAGIC, a training-free framework that achieves motion-aware generation through iterative LLM-guided video generation and differentiable MPM simulation. Our innovations lie in integrating pretrained video generation model and confidence-driven LLM feedback mechanism for physics reasoning optimization in the iteration. We also leverage a real-time MPM engine that simulates multi material behaviors with the guidance of parameters inferred from robust physics reasoning. Extensive experimental results demonstrate that MAGIC significantly improves physical plausibility in dynamic 3D assets, while maintaining high-quality of text-video consistency.

References

- [1] Jad Abou-Chakra, Feras Dayoub, and Niko Sünderhauf. Particlenerf: Particle based encoding for online neural radiance fields. *arXiv preprint arXiv:2211.04041*, 2022.
- [2] Josh Achiam, Steven Adler, Sandhini Agarwal, Lama Ahmad, Ilge Akkaya, Florencia Leoni Aleman, Diogo Almeida, Janko Altschmidt, Sam Altman, Shyamal Anadkat, et al. Gpt-4 technical report. *arXiv preprint arXiv:2303.08774*, 2023.
- [3] Junhao Cai, Yuji Yang, Weihao Yuan, Yisheng He, Zilong Dong, Liefeng Bo, Hui Cheng, and Qifeng Chen. Gic: Gaussian-informed continuum for physical property identification and simulation. *arXiv preprint arXiv:2406.14927*, 2024.
- [4] Junyi Cao, Shanyan Guan, Yanhao Ge, Wei Li, Xiaokang Yang, and Chao Ma. Neuma: Neural material adaptor for visual grounding of intrinsic dynamics. In *NeurIPS*, 2024.
- [5] Siwei Chen, Yiqing Xu, Cunjun Yu, Linfeng Li, and David Hsu. Differentiable particles for general-purpose deformable object manipulation, 2024.
- [6] Zilong Chen, Feng Wang, Yikai Wang, and Huaping Liu. Text-to-3d using gaussian splatting. In *CVPR*, 2024.
- [7] Yilun Du, Yinan Zhang, Hong-Xing Yu, Joshua B Tenenbaum, and Jiajun Wu. Neural radiance flow for 4d view synthesis and video processing. In *ICCV*, 2021.
- [8] Chenfanfu Jiang, Craig Schroeder, Andrew Selle, Joseph Teran, and Alexey Stomakhin. The affine particle-in-cell method. *ACM Transactions on Graphics (TOG)*, 2015.
- [9] Kai Katsumata, Duc Minh Vo, and Hideki Nakayama. A compact dynamic 3d gaussian representation for real-time dynamic view synthesis. In *ECCV*, 2024.
- [10] Bernhard Kerbl, Georgios Kopanas, Thomas Leimkühler, and George Drettakis. 3d gaussian splatting for real-time radiance field rendering. *ACM Transactions on Graphics*, 2023.
- [11] Bernhard Kerbl, Georgios Kopanas, Thomas Leimkühler, and George Drettakis. 3d gaussian splatting for real-time radiance field rendering. *ACM Transactions on Graphics*, 2023.
- [12] LAION-AI. aesthetic-predictor. <https://github.com/LAION-AI/aesthetic-predictor>, 2022. Accessed: 2023-05-01.
- [13] Simon Le Cleac’h, Hong-Xing Yu, Michelle Guo, Taylor Howell, Ruohan Gao, Jiajun Wu, Zachary Manchester, and Mac Schwager. Differentiable physics simulation of dynamics-augmented neural objects. *IEEE Robotics and Automation Letters*, 2023.
- [14] Xuan Li, Yi-Ling Qiao, Peter Yichen Chen, Krishna Murthy Jatavallabhula, Ming Lin, Chenfanfu Jiang, and Chuang Gan. Pac-nerf: Physics augmented continuum neural radiance fields for geometry-agnostic system identification. In *ICLR*, 2023.
- [15] Zhiqi Li, Yiming Chen, and Peidong Liu. Dreammesh4d: Video-to-4d generation with sparse-controlled gaussian-mesh hybrid representation. In *NeurIPS*, 2024.
- [16] Minghui Lin, Xiang Wang, Yishan Wang, Shu Wang, Fengqi Dai, Pengxiang Ding, Cunxiang Wang, Zhengrong Zuo, Nong Sang, Siteng Huang, et al. Exploring the evolution of physics cognition in video generation: A survey. *arXiv preprint arXiv:2503.21765*, 2025.

- [17] Yuchen Lin, Chenguo Lin, Jianjin Xu, and Yadong MU. OmniphysGS: 3d constitutive gaussians for general physics-based dynamics generation. In *ICLR*, 2025.
- [18] Fangfu Liu, Hanyang Wang, Shunyu Yao, Shengjun Zhang, Jie Zhou, and Yueqi Duan. Physics3d: Learning physical properties of 3d gaussians via video diffusion. *arXiv preprint arXiv:2406.04338*, 2024.
- [19] Shaowei Liu, Zhongzheng Ren, Saurabh Gupta, and Shenlong Wang. Physgen: Rigid-body physics-grounded image-to-video generation. In *ECCV*, 2024.
- [20] Zhuoman Liu, Weicai Ye, Yan Luximon, Pengfei Wan, and Di Zhang. Unleashing the potential of multi-modal foundation models and video diffusion for 4d dynamic physical scene simulation. *CVPR*, 2025.
- [21] Miles Macklin. Warp: A high-performance python framework for gpu simulation and graphics. In *NVIDIA GPU Technology Conference (GTC)*, 2022.
- [22] Siwei Meng, Yawei Luo, and Ping Liu. Grounding creativity in physics: A brief survey of physical priors in aigc. *arXiv preprint arXiv:2502.07007*, 2025.
- [23] Qiaowei Miao, Kehan Li, Jinsheng Quan, Zhiyuan Min, Shaojie Ma, Yichao Xu, Yi Yang, and Yawei Luo. Advances in 4d generation: A survey. *arXiv preprint arXiv:2503.14501*, 2025.
- [24] Ben Mildenhall, Pratul P Srinivasan, Matthew Tancik, Jonathan T Barron, Ravi Ramamoorthi, and Ren Ng. Nerf: Representing scenes as neural radiance fields for view synthesis. In *ECCV*, 2020.
- [25] Xiangyu Peng, Zangwei Zheng, Chenhui Shen, Tom Young, Xinying Guo, Binluo Wang, Hang Xu, Hongxin Liu, Mingyan Jiang, Wenjun Li, et al. Open-sora 2.0: Training a commercial-level video generation model in \$200 k. *arXiv preprint arXiv:2503.09642*, 2025.
- [26] Albert Pumarola, Enric Corona, Gerard Pons-Moll, and Francesc Moreno-Noguer. D-nerf: Neural radiance fields for dynamic scenes. In *CVPR*, 2021.
- [27] Alec Radford, Jong Wook Kim, Chris Hallacy, Aditya Ramesh, Gabriel Goh, Sandhini Agarwal, Girish Sastry, Amanda Askell, Pamela Mishkin, Jack Clark, et al. Learning transferable visual models from natural language supervision. In *ICML*, 2021.
- [28] Junuthula Narasimha Reddy. *An introduction to continuum mechanics*. Cambridge university press, 2013.
- [29] Jiawei Ren, Cheng Xie, Ashkan Mirzaei, Karsten Kreis, Ziwei Liu, Antonio Torralba, Sanja Fidler, Seung Wook Kim, Huan Ling, et al. L4gm: Large 4d gaussian reconstruction model. In *NeurIPS*, 2024.
- [30] Alvaro Sanchez-Gonzalez, Jonathan Godwin, Tobias Pfaff, Rex Ying, Jure Leskovec, and Peter W. Battaglia. Learning to simulate complex physics with graph networks. In *ICML*, 2020.
- [31] Xiyang Tan, Ying Jiang, Xuan Li, Zeshun Zong, Tianyi Xie, Yin Yang, and Chenfanfu Jiang. Physmotion: Physics-grounded dynamics from a single image. *arXiv preprint arXiv:2411.17189*, 2024.
- [32] Jiaxiang Tang, Zhaoxi Chen, Xiaokang Chen, Tengfei Wang, Gang Zeng, and Ziwei Liu. Lgm: Large multi-view gaussian model for high-resolution 3d content creation. In *ECCV*, 2024.
- [33] Zachary Teed and Jia Deng. Raft: Recurrent all-pairs field transforms for optical flow. In *ECCV*, 2020.
- [34] Vikram Voleti, Chun-Han Yao, Mark Boss, Adam Letts, David Pankratz, Dmitry Tochilkin, Christian Laforte, Robin Rombach, and Varun Jampani. Sv3d: Novel multi-view synthesis and 3d generation from a single image using latent video diffusion. In *ECCV*, 2024.
- [35] Jianfeng Xiang, Zelong Lv, Sicheng Xu, Yu Deng, Ruicheng Wang, Bowen Zhang, Dong Chen, Xin Tong, and Jiaolong Yang. Structured 3d latents for scalable and versatile 3d generation. *arXiv preprint arXiv:2412.01506*, 2024.
- [36] Tianyi Xie, Zeshun Zong, Yuxing Qiu, Xuan Li, Yutao Feng, Yin Yang, and Chenfanfu Jiang. Physgaussian: Physics-integrated 3d gaussians for generative dynamics. In *CVPR*, 2024.
- [37] Qingshan Xu, Jiao Liu, Melvin Wong, Caishun Chen, and Yew-Soon Ong. Precise-physics driven text-to-3d generation. *arXiv preprint arXiv:2403.12438*, 2024.
- [38] Zhuoyi Yang, Jiayan Teng, Wendi Zheng, Ming Ding, Shiyu Huang, Jiazheng Xu, Yuanming Yang, Wenyi Hong, Xiaohan Zhang, Guanyu Feng, et al. Cogvideox: Text-to-video diffusion models with an expert transformer. In *ICLR*, 2025.

- [39] Jingyang Zhang, Yao Yao, and Long Quan. Learning signed distance field for multi-view surface reconstruction. In *ICCV*, 2021.
- [40] Tianyuan Zhang, Hong-Xing Yu, Rundi Wu, Brandon Y Feng, Changxi Zheng, Noah Snavely, Jiajun Wu, and William T Freeman. Physdreamer: Physics-based interaction with 3d objects via video generation. In *ECCV*, 2024.
- [41] Licheng Zhong, Hong-Xing Yu, Jiajun Wu, and Yunzhu Li. Reconstruction and simulation of elastic objects with spring-mass 3d gaussians. In *ECCV*, 2024.
- [42] Zeshun Zong, Xuan Li, Minchen Li, Maurizio M Chiaramonte, Wojciech Matusik, Eitan Grinspun, Kevin Carlberg, Chenfanfu Jiang, and Peter Yichen Chen. Neural stress fields for reduced-order elastoplasticity and fracture. In *SIGGRAPH Asia 2023 Conference Papers*, 2023.